Effects of Plastic Deformation on Fatigue Life of Superduplex Steel Tube Umbilical

Conference Paper · July 2012

DOI: 10.1115/OMAE2012-83204

Diego F. B. Sarzosa
University of São Paulo

Rafael Savioli
University of São Paulo

Gustavo Donato
University Center of FEI

Claudio Ruggieri
University of São Paulo

Proceedings of the ASME 31st International Conference on Offshore Mechanics and Arctic Engineering
OMAE2012
July 1-6, 2012, Rio de Janeiro, Brazil

OMAE2012-83204

EFFECTS OF PLASTIC DEFORMATION ON FATIGUE LIFE OF SUPERDUPLEX STEEL TUBE UMBILICAL

Diego F. S. Burgos
Dept. of Naval Arch. and Ocean Eng.
University of São Paulo
São Paulo, SP 05508-900, Brazil

Luís F. S. Parise
Dept. of Naval Arch. and Ocean Eng.
University of São Paulo
São Paulo, SP 05508-900, Brazil

Rafael G. Savioli
Dept. of Naval Arch. and Ocean Eng.
University of São Paulo
São Paulo, SP 05508-900, Brazil

Gustavo H. B. Donato
Dept. of Mech. Eng.
FEI University Center
S. B. Campo, SP 09850-901, Brazil

Antonio P. Nascimento Filho
Surflex Umbilicais e Tubos Flexíveis do Brasil Ltda.
Vila Velha, ES 29114-035, Brazil

Carlos A. Lemos
Petrobras Research Center
CENPES
Rio de Janeiro, RJ 21941-915, Brazil

Neilon Silva
Petrobras Research Center
CENPES
Rio de Janeiro, RJ 21941-915, Brazil

Claudio Ruggieri
Dept. of Naval Arch. and Ocean Eng.
University of São Paulo
São Paulo, SP 05508-900, Brazil

ABSTRACT
This work presents an experimental investigation of the effects of plastic strain on the fatigue behavior of superduplex steel tubes. Fatigue tests using conventional axial loading and a resonant bending setup conducted on 15mm OD tubes made of SAF2507 superduplex steel provides $S \times N$ data upon which effects of different levels of plastic strain can be assessed. Despite the inherent scatter in the measured fatigue data, the experiments reveal consistent trends and relatively small effects of plastic strain on fatigue behavior of superduplex steel tubes.

INTRODUCTION
Small diameter steel tubes made of duplex and superduplex materials are a key component in deep water umbilical structures. As the offshore infrastructure moves into even deeper waters, the umbilical structure is subjected to more severe and complex conditions, including high external hydrostatic pressure coupled with high dynamic environmental loads. Fatigue caused by cyclic tension and bending associated with the umbilical structure reacting to vessel motion and variable amplitude loading from sea waves and current actions represents the most common and significant failure mechanism. Consequently, a critical step in design, installation and safe

operation of deep water umbilical cables lies in accurate assessments of the fatigue life for these steel tubes, particularly their girth welds.

Current design and in-service fatigue assessments for welded components and circumferentially welded pipes, such as DNV procedures [1,2] and Eurocode [3], employ conventional methodologies adopting stress-life approaches in which fatigue life predictions are made based upon reference fatigue curves and the simple knowledge of nominal stresses acting on the weldment. While used effectively in many structural applications, it does not consider properly the potential deleterious effects of plastic strain on the fatigue life and fatigue limit. For umbilical cables installed by the reeling process, the steel tubes are subjected to large straining and plastic deformation levels (2 ~3%) well beyond the materials elastic limits. This large, localized plastic deformation may potentially cause severe material damage with significant reduction in fatigue life, particularly in the girth weld region [4-6]. Consequently, advanced procedures for fatigue assessments of steel tube umbilicals must include the effects of plastic deformation that arise during reeling installation on fatigue life predictions for umbilical structures.

As a step in this direction, this work presents an experimental investigation of the effects of plastic strain on the fatigue behavior of superduplex steel tubes. Fatigue tests using conventional axial loading and a resonant bending setup conducted on 15 mm OD tubes made of SAF2507 superduplex steel provide $S \times N$ data upon which effects of different levels of plastic strain can be assessed. Despite the inherent scatter in the measured fatigue data, the experiments reveal consistent trends and relatively small effects of plastic strain on fatigue behavior of superduplex steel tubes.

EXPERIMENTAL PROGRAM

Materials and Test Specimens

A series of high-cycle fatigue tests were performed on welded and unwelded steel tube umbilicals (STUs) specimens. The material utilized in this study is a high alloy superduplex stainless steel SAF 2507 used in metallic tubes contained in the umbilical cable structure. For the welded tubular specimens, the girth welds are prepared using a mechanized orbital GTAW procedure.

The high-cycle fatigue tests were conducted on two different specimen configurations which include: 1) small-size, unwelded tubular specimens designed for conventional uniaxial fatigue testing having outside diameter, D_e = 15.6 mm, with wall thickness, t = 1.4 mm and overall length, l_e = 215 mm (which includes the grip region) and 2) full-scale, straight section welded specimens designed for bending fatigue testing using a resonant test device developed by University of São Paulo and Petrobras. Here, two similar sets of 1000 mm long tubular specimens were utilized for the fatigue testing: *i*) D_e = 15.6 mm, with wall thickness, t = 1.4 mm and *ii*) D_e = 14.7 mm, with wall thickness, t = 1.0 mm. Figure 1 displays a schematic illustration of the geometry and dimensions of the unwelded tubular specimens employed in the uniaxial fatigue testing which follows similar arrangement adopted by Bose and Spinelli [7] building on recommendations for tensile testing of tubular specimens given by ASTM E8 [8] and ASTM A370 [9].

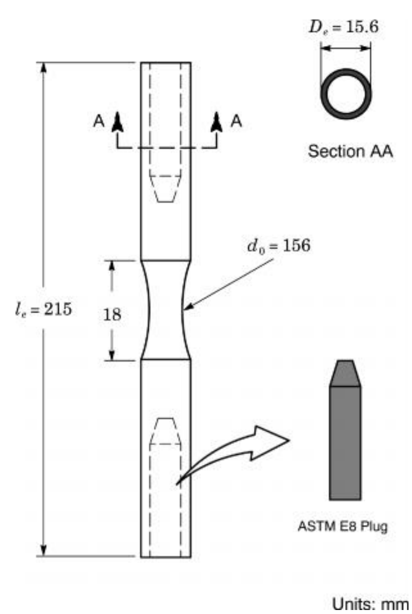

Figure 1. Small-size, unwelded tubular specimens designed for conventional uniaxial fatigue testing.

Fatigue Test Procedures

The high-cycle fatigue experiments for the unwelded tubular specimens were performed on an MTS servo-hydraulic testing machine at a frequency of 10 Hz (sine wave) under load control and constant amplitude loading with ratio, R = -1. Because these specimens are unwelded, much higher levels of stress range are expected at failure for a given number of cycles; here, the stress ranges are selected between ~800 and 1200 MPa. Further, to verify the potential strong effects of plastic deformation on the fatigue lives for theses specimens, three levels of plastic strains are considered in the fatigue test: 0% (virgin or as-received material), 2% and 6%. These levels of plastic strain were achieved by imposing a uniaxial (tensile), uniform elongation on the specimens such as the desired residual (plastic) strain is attained after unloading. Figure A1(a) in Annex A shows the test setup for the uniaxial fatigue testing. Figure A1(b) displays a closer view of the small-sized tubular specimen.

Fatigue testing of the welded tubular specimens was conducted using a resonant test device at a frequency of 30 Hz with a cyclic constant bending load such as the resulting stress range (load ratio, R = -1) varied from 400 to 700 MPa. To simulate the reeling condition that arises from manufacture and installation operations of the umbilicals, a longitudinal plastic strain history was applied in one set of these tubular specimens as follows. First, the specimen is bent over a custom-designed, steel bending grooved shoe to a 2% strain. Next, the specimen is twisted about their longitudinal axis while keeping the shoe curvature unchanged so that all material points over the tube cross section are subjected to an essentially similar strain history. By twisting the tubular specimens a given number of turns, a cumulative reeling strain can be attained. Here, the specimens are twisted 2.25 turns giving rise to a 20% accumulated plastic strain (APS). The procedure for applying the APS on the welded tubular specimens follows closely the methodology discussed by Buitrago et al [5,6]. Figure A2(a) in Annex A displays the resonant fatigue test setup including a 1-m welded tubular specimen mounted and instrumented for testing. Figure A2(b) depicts a detail of the custom-designed, steel bending grooved shoe utilized to apply a predefined strain as a function of the curvature. Figure A2(c) displays a closer view of the welded tubular specimen used in the resonant fatigue testing.

EXPERIMENTAL RESULTS

Tensile Test Data

Figure 2 displays the measured tensile response of the tested SAF 2507 steel tubing (average of three tensile tests) at room temperature for the unwelded condition which also includes the engineering and the true stress ($\bar{\sigma}$) *vs.* true strain ($\bar{\varepsilon}$) data. The (tubular) tensile specimens were extracted directly from the long, straight delivered tubing sections and machined according to the specifications given by ASTM E8M [8]. Table 1 summarizes the mechanical properties obtained from the tensile tests (average of three tests). The tested material has 715 MPa yield stress (σ_{ys}) with relatively-high to moderate hardening behavior ($\sigma_{uts}/\sigma_{ys} \approx$ 1.35); here, σ_{uts} denotes the ultimate tensile strength. Other mechanical properties for the material include Young's modulus, E = 201 GPa, Poisson's ratio, υ = 0.3, and failure strain, $\varepsilon_f = 0.365$.

To facilitate further interpretation of the flow characteristics of the tested SAF 2507 steel, the above Table 1 also includes the Ramberg-Osgood exponent, *n*, derived from fitting the true stress ($\bar{\sigma}$) *vs.* true strain ($\bar{\varepsilon}$) data from the following equation provided by Annex F of API 579 as [10]

$$\bar{\varepsilon} = \frac{\bar{\sigma}}{E} + \left(\frac{\bar{\sigma}}{H}\right)^n \qquad (1)$$

in which H is a fitting constant dependent upon σ_{uts} and *n*.

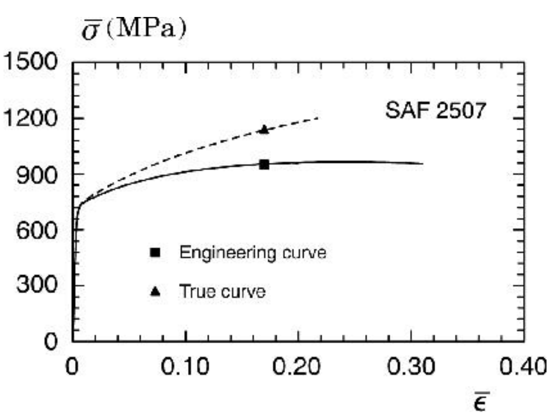

Figure 2. Measured tensile behavior of the tested SAF 2507 steel tubing including the true stress-true strain data.

Table 1. Material properties of the tested SAF 2507 steel.

σ_{ys} (MPa)	σ_{uts} (MPa)	n	ε_f
715	965	9.8	0.365

Uniaxial Fatigue Test Results

This section describes key results which primarily serve to examine the effects of prestrain on the fatigue life for the unwelded tubular specimen. Because the uniaxial test provides a much better control of loading, applied uniaxial strain and gripping conditions, among other test variables, these experimentally measured fatigue curves can be interpreted as "baseline" curves in the present context.

Consider first the fatigue test data for the virgin material (0% prestrain) displayed in Fig. 3 in terms of stress range, ΔS, *vs.* number of cycles to failure , N_f. The solid symbols represent the measured fatigue data. The straight lines define fitting curves derived from a best fit to the experimental data set, including the curve for the mean minus two standard deviation (which corresponds to a 97.6% survival probability [1]). To facilitate comparison, this plot also includes the $S \times N$ curve specified by DNV C203 [1] for girth welds of small diameter umbilicals. As could be anticipated, the unwelded material has a much higher fatigue life than the $S \times N$ curve provided by DNV C203 [1].

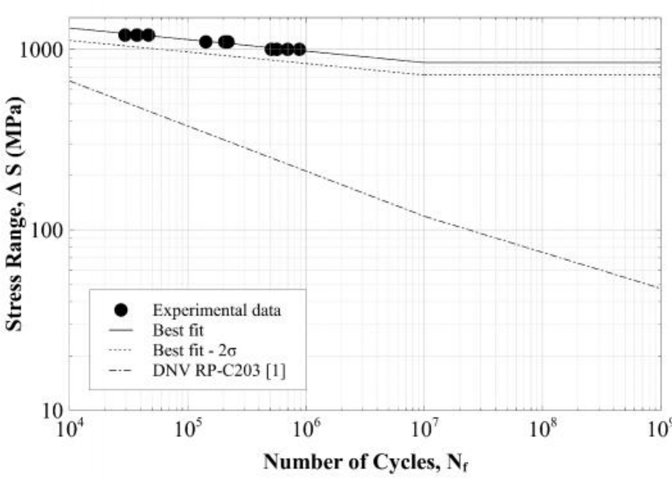

Figure 3. Fatigue life in terms of stress range, ΔS, versus number of cycles to failure , N_f, for the SAF 2507 unwelded tubular specimens in the as-received condition (0% prestrain).

Now consider the dependence of fatigue life on the level of prestrain for the unwelded tubular specimens for different levels of plastic strain: 0% (virgin or as-received material), 2% and 6% shown in Fig. 4. Again, the solid symbols represent the measured fatigue data whereas the straight lines correspond to a best fit derived from a linear least square fitting to the experimental data. Here, Fig. 4(a) displays the fatigue curves over a wide range of N_f (from 10^4 to 10^9 cycles) and Fig 4(b) shows a closer view of the fatigue plots in the range $10^4 \le N_f \le 10^6$.

As could be expected, it is found that increasing the level of applied prestrain brings about a reduction in the fatigue life for the tubular specimens. However, the fatigue test data for the tested specimens appears to display only a relatively small sensitivity on the level of plastic strain. Because of the inherent large scatter of the experimental data, it is helpful to limit attention to the best fit curves when proceeding with the interpretation of the results. Observe that the reduction in fatigue life is much more prominent for 2% prestrain than the much higher 6% prestrain, particularly at longer fatigue lives. For a given level of stress range (say, 1000 MPa), the fatigue life decreases more rapidly for the 2% prestrain level and then more slowly as the level of prestrain is increased to 6%. We also note that, as the stress range, ΔS, is increased (*i.e.*, higher stress ranges), the effect of prestrain on fatigue life is even smaller. Such behavior can be partly explained in terms of plasticity development in the specimen cross section (associated with the larger strains) which relieves the effects of large plastic strains thereby offsetting the influence of prestrain.

Resonant Fatigue Test Results

Analogously to the previous section, Figure 5 shows the effect of prestrain on the fatigue life (expressed as log ΔS *vs.* log N_f where ΔS is the stress range and N_f denotes the number of cycles to failure) for the welded tubular specimens (subjected to reeling) for different levels of plastic strain: 0% (virgin or as-received material) and 20% APS. Unfortunately, only few experimental points are available for the welded tubular specimens subjected to 20% APS; additional testing is currently underway to construct a more complete fatigue life curve, including other levels of APS. In this plot, the solid symbols represent the measured fatigue data whereas the straight lines correspond to a best fit derived from a linear least square procedure to the experimental data. To facilitate comparison, Figure 5 also includes the fatigue life curve for similar welded tubular specimens subjected to a 20% APS prestrain tested by Buitrago et al. [6] as well as the $S \times N$ curve provided by DNV C203 [1].

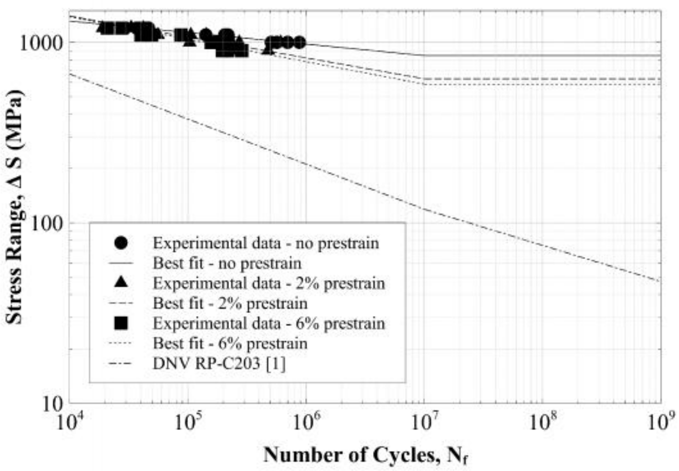

(a)

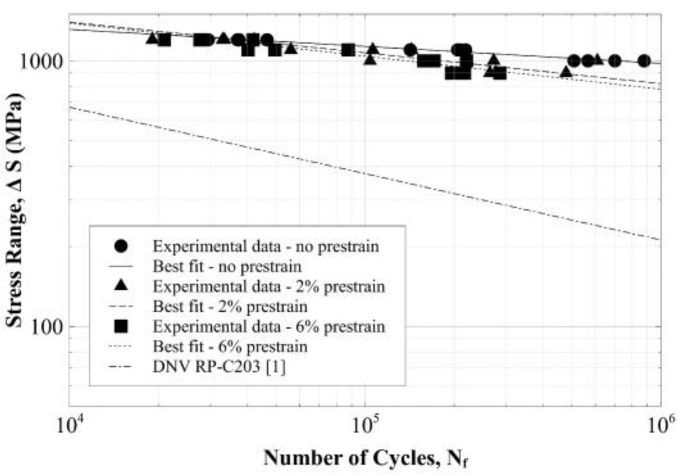

(b)

Figure 4. Fatigue life in terms of stress range, ΔS, versus number of cycles to failure, N_f, for the SAF 2507 unwelded tubular specimens with varying levels of applied prestrain.

Despite only few data points available, these results allow examining the effects of prestrain on the fatigue life for the welded tubular specimens. Again, because of the inherent large scatter of the experimental data, it is helpful to limit attention to the best fit curves in proceeding with the analysis of these results. Observe that the best fit curve for the 20% APS condition lie below the corresponding curve for the unstrained tubular specimen (0% prestrain) thereby also shifting the fatigue limit (which corresponds to the stress range at $N_f = 10^7$ cycles in the present context). Perhaps more importantly, the entire set of fatigue test data (0% prestrain and 20% APS) are well above the fatigue design curve provided by DNV C-203 [1], particularly for shorter fatigue lives ($N_f \leq 10^5$ cycles). Note, however, that differences in the fatigue limit for all sets analyzed are relatively smaller.

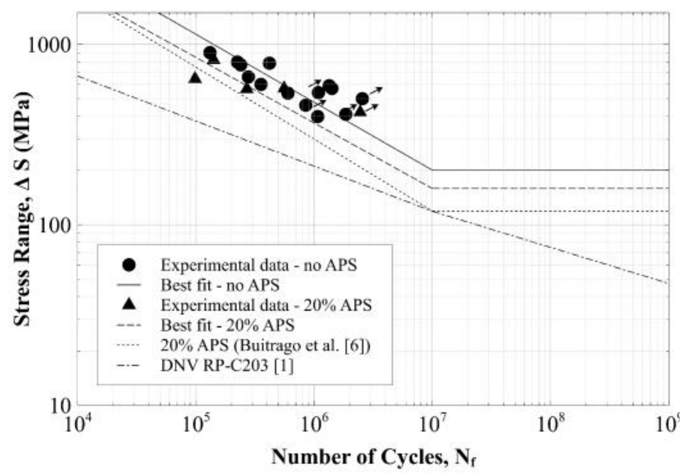

Figure 5. Fatigue life in terms of stress range, ΔS, versus number of cycles to failure, N_f, for the SAF 2507 welded tubular specimens (subjected to reeling) with varying levels of applied prestrain.

Moreover, compared to the fatigue life curve for the unwelded tubular specimen, a significant reduction in the stress range at a given number of cycles at failure can be observed. Such feature is an obvious result but emphasizes the prominent role of the girth weld on the fatigue life of steel tubing for umbilicals. Due to the limited data set available at this moment (as already observed, additional testing is underway), no attempt was made now to determine the confidence bands for the fatigue test data. A detailed statistical analysis will be pursued upon completion of all tests with different levels of APS.

CONCLUDING REMARKS

An experimental investigation of the effects of plastic strain on the fatigue behavior of superduplex steel tubes was conducted. Fatigue tests using conventional axial loading and a resonant bending setup conducted on 15 mm OD tubes made of SAF2507 superduplex steel provide the $S \times N$ data upon which effects of different levels of plastic strain can be assessed. Despite the inherent scatter in the measured fatigue data, the experiments reveal consistent trends and relatively small effects of plastic strain on fatigue behavior of superduplex steel tubes.

In interpreting the results presented in this article to discuss a proper influence of plastic strain, particularly the effects of APS levels, on the fatigue life of superduplex steel tubes, it is well to keep in mind the actual response of the material when subjected to different levels of plastic deformation. Indeed, the concept of accumulated plastic strain (APS) may be simply viewed as a plastic *cyclic* loading in which the direction of straining is reversed after a certain level of yielding has occurred (for example, 2%). Because the number of cycles is very small (usually less than ~10 cycles), the material response will most likely follow a stable stress-strain hysteresis loop, *i.e.*, a stable cyclic stress-strain curve. Dowling [11] provides a detailed presentation on the cyclic loading behavior of material. Consequently, the plastic strain levels effectively acting on the welded tubular specimens (in which a 20% APS was applied) correspond to 2%.

Additional work is in progress to test and construct more complete fatigue life curves for welded tubular specimens at different levels of APS, including the statistical confidence intervals. Ongoing investigation also focuses on the numerical simulation of the reeling of the small steel tubings to clarify the actual role of APS on the plastic deformation history and fatigue life.

ACKNOWLEDGMENTS

This investigation is supported by the Brazilian State Oil Company (PETROBRAS). The authors acknowledge Surflex Umbilicais e Tubos Flexíveis do Brasil (Prysmian) for providing the tubular specimens made of SAF 2507 superduplex steel.

REFERENCES

[1] Det Norske Veritas, "Fatigue Design of Offshore Steel Structures", Recommended Practice DNV-RP-C203, 2011.

[2] Det Norske Veritas, "Fracture Control for Pipeline InstallationMethods Introducing Cyclic Plastic Strain", Recommended Practice DNV-RP-F108, 2006.

[3] European Committee for Standardization, "Eurocode 3: Design of Steel Structures − Part 1-9: Fatigue", EN1993-1-9, Brussels, 2005.

[4] Kristoffersen, S. and Haagensen, P. J., "Fatigue Design Criteria for Small Super Duplex Steel Pipes", Proceedings of Offshore Mechanics and Arctic Engineering Conference (OMAE 2004), Vancouver, 2004.

[5] Buitrago, J., Doyonov, K. and Fox, A., "Effect of Reeling on Welded Umbilical Tubing Fatigue", Proceedings of Offshore Mechanics and Arctic Engineering Conference (OMAE 2006), Hamburgo, 2006.

[6] Buitrago, J., Doyonov, K. and Fox, A., "Effect of Reeling on Small Umbilical Tubing Fatigue", Proceedings of Offshore Mechanics and Arctic Engineering Conference (OMAE 2008), Estoril, 2008.

[7] Bose, W. W. and Spinelli, D., *Private Communication*, 2010.

[8] American Society for Testing and Materials, "Standard Test Methods for Tension Testing of Metallic Materials", ASTM E8M, 2009.

[9] American Society for Testing and Materials, "Standard Test Methods and Defnitions for Mechanical Testing of Steel Products", ASTM A 370, 2009.

[10] American Petroleum Institute. "Fitness-for-Service", API RP-579-1 / ASME FFS-1, 2007.

[11] Dowling, N. E., "Mechanical Behavior of Materials: Engineering Methods for Deformation, Fracture and Fatigue." 3rd Ed., Prentice Hall, New Jersey, 2005.

ANNEX A

FATIGUE TESTING

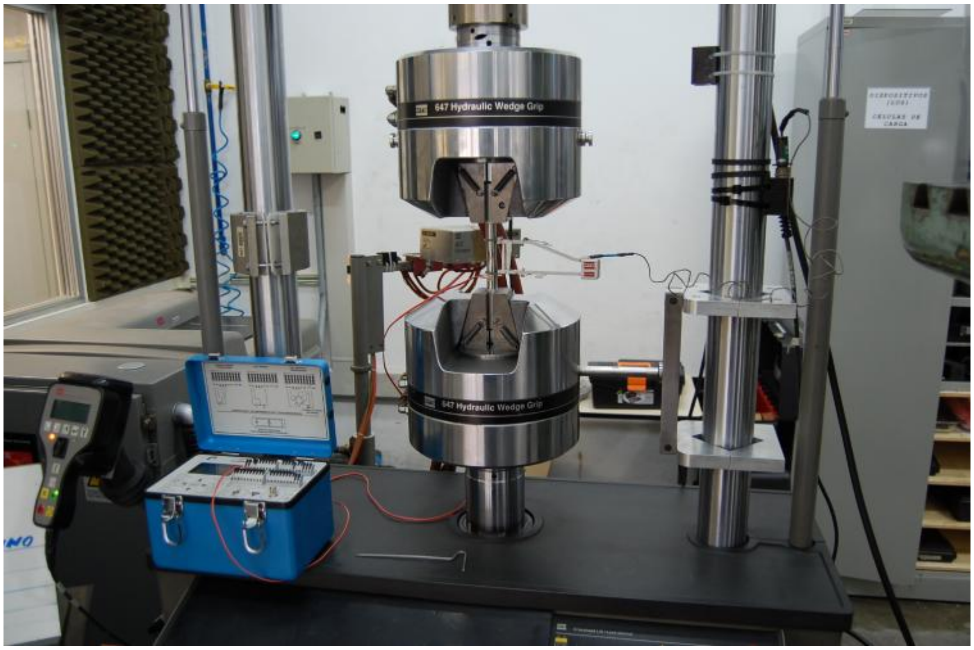

(a)

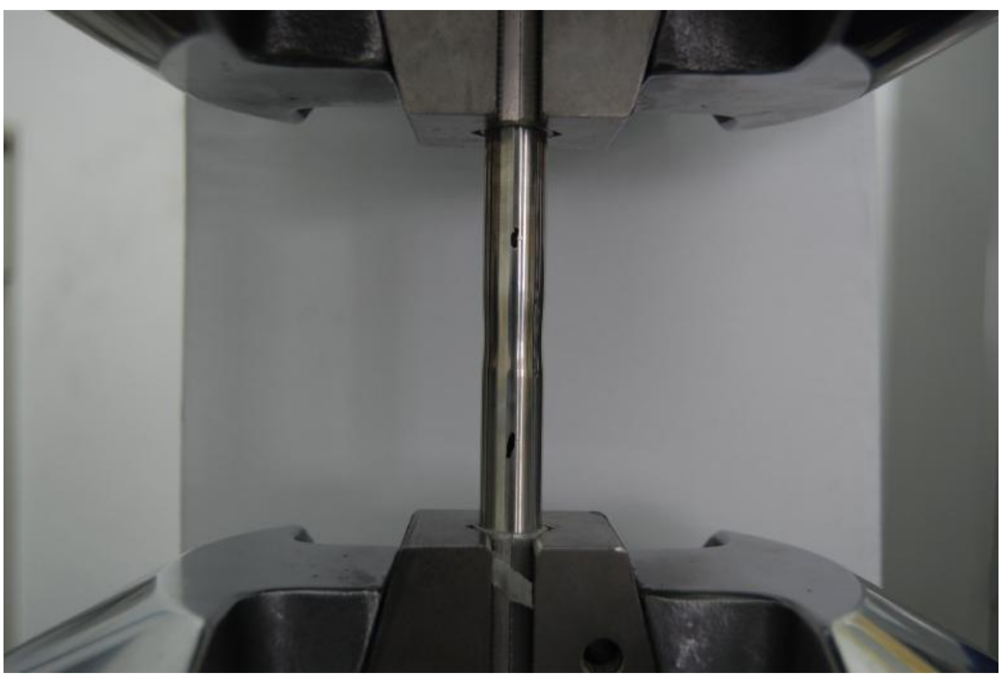

(b)

Figure A1. (a) Test setup for uniaxial fatigue testing. **(b)** Close-up of mounted specimen utilized for uniaxial fatigue testing.

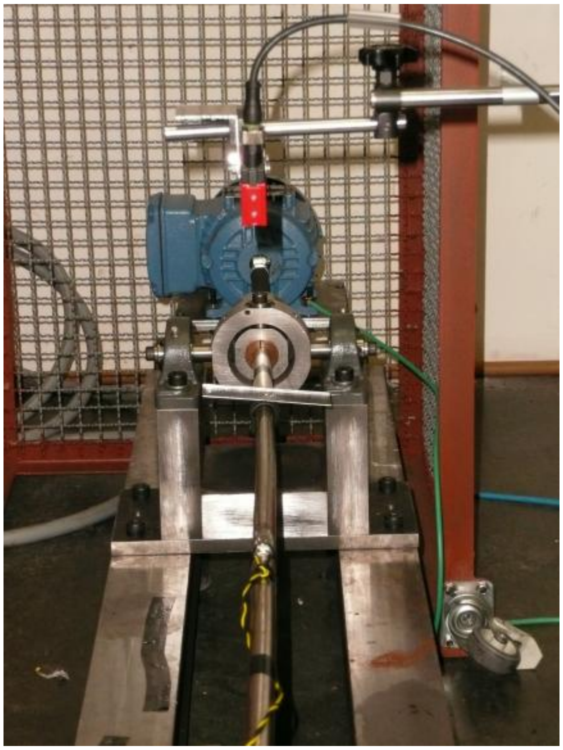

(a)

(b)

(c)

Figure A2. (a) Test setup for resonant fatigue testing. **(b)** Detail of custom-designed, steel bending grooved shoe utilized to apply the APS. **(c)** Close-up of mounted welded specimen utilized for resonant fatigue testing.

